Neuro-Oncology 13(6):610–621, 2011.
doi:10.1093/neuonc/nor035

Control of proliferation in astrocytoma cells by the receptor tyrosine kinase/PI3K/AKT signaling axis and the use of PI-103 and TCN as potential anti-astrocytoma therapies

Demirkan B. Gürsel†, Yvette S. Connell-Albert†, Robert G. Tuskan, Theonie Anastassiadis, Jessica C. Walrath, Jessica J. Hawes, Jessica C. Amlin-Van Schaick, and Karlyne M. Reilly

Mouse Cancer Genetics Program, Center for Cancer Research, National Cancer Institute-Frederick, Frederick, MD (D.B.G., Y.S.C.-A., R.G.T., T.A., J.C.W., J.J.H., J.C.A.-V.S., K.M.R.); Molecular Biology and Microbiology, George Mason University, Fairfax, VA (Y.S.C.-A.)

A growing body of work suggests that astrocytomas and glioblastoma multiforme will require carefully tailored, molecularly targeted therapy for successful treatment. Recent efforts to comprehensively identify mutations and gene expression changes in glioblastoma have shown that mutation of *NF1* is a common alteration in human glioblastoma. We have developed and characterized a panel of 14 tumor lines from grades II through IV astrocytomas developed from our *Nf1−/+; Trp53−/+cis* mouse model and have used this panel to characterize signal transduction pathways and inhibitors that are candidate therapeutic targets for astrocytoma and glioblastoma. We show that these tumors express platelet-derived growth factor receptor–α, epidermal growth factor receptor, and their respective ligands to varying degrees. We find that both the MEK and PI3K signaling pathways downstream of epidermal growth factor receptor and platelet-derived growth factor receptor–α are necessary for full proliferation of astrocytoma cells; however, inhibition of the PI3K pathway is more effective than inhibition of MEK at blocking cell growth. We have examined inhibitors of the PI3K/Akt/mTOR signaling pathway and find that PI-103 and TCN show particular promise for inhibiting growth in *Nf1* and *Trp53* mutant astrocytoma cells.

Keywords: Akt, astrocytoma, EGFR, Nf1, p53.

Malignant astrocytomas, which include diffuse astrocytoma (World Health Organization [WHO] grade II), anaplastic astrocytoma (WHO III), and glioblastoma multiforme (GBM) (WHO IV), are the most common and deadly brain tumors in adults.[1] These tumors are currently incurable, with very little improvement in prognosis over the past decade. Efforts to develop chemotherapy have extended survival modestly in some cases but have failed to cure the disease.[2] With the identification of targetable signal transduction pathways involving epidermal growth factor receptor (EGFR) and platelet-derived growth factor receptor (PDGFR) in brain tumors, molecularly targeted therapies have entered clinical trials for brain tumors (http://clinicaltrials.gov/) but have not been as successful as hoped.[3,4] Careful analyses of completed clinical trials have demonstrated that although the molecularly targeted therapies may not have efficacy across all brain tumor patients tested, a subset of patients with particular tumor molecular signatures are very responsive to therapy.[5,6] This suggests that molecularly targeted therapies may need to be tested in very focused clinical trials to show efficacy and highlights the importance of studying candidate therapies in a wide variety of model systems with specific, well-defined mutations.

Receptor tyrosine kinases (RTKs) are frequently dysregulated in astrocytomas and GBMs (see review[7]). Two

Received August 20, 2010; accepted February 25, 2011.

Present affiliation: Department of Neurological Surgery, Weill Cornell Medical College, New York, USA (D.B.G.).

†These authors contributed equally to this work.
Corresponding Author: Karlyne M. Reilly, Ph.D., West 7th St at Fort Detrick, PO Box B, Frederick, MD 21702 (kreilly@ncifcrf.gov).

such RTKs, EGFR and PDGFRα, play important roles in the development of many cancers, as well as in diverse cellular processes, including proliferation, differentiation, and migration. EGFR expression is upregulated through amplification, mutation, and rearrangement in GBMs, whereas PDGFRα is overexpressed at the transcriptional level. Ligands to these receptors are also overexpressed in astrocytomas, giving rise to autocrine loops that may contribute to the oncogenicity of these tumors. Two of the main signaling pathways stimulated through activation of EGFR and PDGFRα are for phosphatidylinositol 3-kinase (PI3K) and mitogen-activated protein/extracellular signal-regulated kinase (MEK). In humans, the PI3K pathway has been shown to be dysregulated in GBM,[8] and a high percentage of GBMs show Akt activation downstream of PI3K.[9] In addition, gain of function mutations in PI3K have been seen in many cancers.[10] Previous studies have also shown that an increase in activated Akt and mitogen-activated protein kinase (MAPK), downstream of MEK, correlates with the progression of astrocytoma to GBM.[11]

The p53 protein is a critical tumor suppressor involved in cell cycle arrest for the maintenance of genomic integrity.[12] The *Tp53* gene (*Trp53* in mice) encoding p53 is frequently lost or mutated in astrocytomas and GBMs (see review[7]). The p53 pathway can be lost in astrocytoma/GBM through direct loss/mutation of the *Tp53* gene, through loss/mutation of the upstream regulator *p14ARF*, or by amplification of the p53 inhibitor *MDM2*. Although the p53 pathway is mutated in most if not all GBMs, mutation of the *Tp53* gene itself is negatively correlated with amplification of *EGFR*,[13] but is often found with overexpression of *PDGFRα*.

Neurofibromin is a tumor suppressor that acts to downregulate active Ras and is encoded by the *NF1* gene (*Nf1* in mice). Recent efforts to completely sequence genes from large numbers of sporadic GBMs have demonstrated that *NF1* carries point mutations in 14%–15% of GBMs,[13,14] with an additional 9% showing deletion of the *NF1* gene.[13] Similar to *Tp53*, alterations in *NF1* show negative association with amplification or mutation of *EGFR*.[13] However, both *EGFR* and *PDGFRα* are overexpressed at the transcriptional level in tumors with reduced expression of or mutations in *NF1*.[14]

We have developed a mouse model of astrocytoma in which the *Nf1* gene and the *Trp53* gene are mutated together on the same chromosome in *cis* (*NPcis* mice).[15] We previously demonstrated that the incidence of astrocytomas in this model is dependent on genetic and epigenetic factors.[16] Here we present a panel of tumor cell lines from this model that can be used to study the biology of *Nf1* and *Trp53* mutant tumor cells of different grades in vitro and may eventually help us to understand the role of susceptibility factors in cancer. Furthermore, we describe the characterization of these tumor lines with respect to RTKs and downstream signaling pathways, and we use these tumor lines in preclinical studies of candidate therapeutics to compare the efficacy of inhibiting different signaling pathways in blocking tumor cell proliferation, anchorage-independent growth, and migration.

Materials and Methods

Breeding and Genotyping of NPcis *Mice*

NPcis mice were bred on inbred C57BL/6J and 129S4/SvJae backgrounds, as described previously,[16] at the National Cancer Institute (NCI) in Frederick, Maryland. All mice used for tumor lines were bred either from mutant mothers crossed to wild-type (WT) fathers or from WT mothers crossed to mutant fathers, so that the parental source of the *NPcis* chromosome is known. Genotyping of mice was performed as described previously.[16] All mouse procedures were performed according to guidelines of the NCI-Frederick Animal Care and Use Committee.

Immunohistochemistry of Primary Tumors

Paraffin sections of brains fixed with Bouin's solution and stained with hematoxylin-eosin were scored for tumor morphology and grade by K.M.R. Paraffin sections of formalin-fixed contralateral halves were immunostained using standard techniques (see Supplementary Methods for details). Primary antibodies used were rabbit anti-EGFR (Cell Signaling cat #2232; 1:50 dilution for chromagenic detection with 3,3'-diaminobenzidine [DAB] and 1:10 for fluorescent detection) and rabbit anti-PDGFRα (Cell Signaling cat #3164; 1:25 dilution for chromogenic detection with DAB and 1:5 for fluorescent detection) or rat anti-PDGFRα (RDI cat #MCD140AabRT; 1:100 for chromogenic detection with DAB). A human brain tumor tissue array (Clinomics LD-BRN-1 #47012703.2) was similarly stained with anti-EGFR and anti-PDRGRα antibodies. Slides were costained using fluorescent techniques with rat anti-Ki67 (Dako, cat #M7249; 1:5).

Generation and Characterization of Tumor Lines and Primary Astrocytes

To establish tumor lines, one sagittal half of the brain was fixed for pathology and the remaining half was cut into ~4-mm^2 pieces, with the location of dissected pieces recorded relative to the sagittal plane (Fig. 1). Tumor lines were established from pieces as described previously[16] in 12-well plates. Lines were maintained in complete media (Dulbecco's modified Eagle medium [Invitrogen] containing 10% fetal bovine serum [FBS; Hyclone] and 1% penicillin-streptomycin [Invitrogen]). Primary astrocytes were made as described previously.[17]

Western Blotting

Cells were lysed in cell lysis buffer (cat #9803 Cell Signaling Technology) with 1 mM phenylmethanesulfonyl fluoride at 90%–100% cell confluency. Total protein (30–40 μg) was separated by 6% sodium dodecyl sulfate polyacrylamide gel electrophoresis

(SDS-PAGE) and analyzed by Western blot for EGFR (cat # 2232B), PDGFR-α (cat # sc-338), Actin (cat #sc-7210) (1:1000; Santa Cruz Biotechnology), and β-tubulin (1:1000; cat #32-2600 Zymed Laboratories). Protein levels were detected with horseradish peroxidase–conjugated secondary antibodies and Enhanced Chemiluminescent Plus (ECL; GE Healthcare) and were quantified using National Institutes of Health ImageJ software (www.nihimagej.com).

To measure phosphorylation changes in Akt and MAPK, cells were grown to 80%–90% confluency and stimulated for 5–10 min with 1–10 ng/mL of epidermal growth factor (EGF; cat #01-107) or platelet-derived growth factor (PDGF)–AA (cat #01-309) (Upstate Biotechnology) with or without 10–20 μM of U0126 (cat #EI-282) or LY-294002 (cat #ST-420) (Biomol Research Lab). Protein lysates (5–20 μg) were separated by 12%–15% SDS PAGE and analyzed by Western blot for Akt (cat #cs-9272), phosphorylated Akt (phospho-Ser 473; cat #cs-9271), MAPK (cat #cs-9102), and phosphorylated MAPK (p44/42 phospho-Thr202/Tyr204; cat #cs-01-9101) antibodies (1:1000; Cell Signaling Technology).

Cell Proliferation Assays

Cells were plated at 5×10^4/35 mm plate and grown in 0, 1, or 10% FBS. Cells were pretreated with LY294002 (20 μM) or U0126 (10 μM) and stimulated with 10 ng/mL of EGF or PDGF-AA. Medium containing fresh inhibitors and ligands was added every 2 days, and cells were counted in duplicate every other day.

Subcutaneous and Intracranial Growth of Tumor Lines

One million astrocytoma cells were injected subcutaneously into athymic mice in quadruplicate. Tumor length and width were measured by caliper every week for 4 weeks, starting when tumors were clearly palpable, to examine long-term growth; or tumor length, width, and height were measured every other day for 20 days from the day of injection to examine short-term growth. Tumor volume was approximated with the equation volume=$(LXW^2)/2$ or volume=(LXWXH)/2 (depending on whether measurements were taken in 2 or 3 dimensions) and plotted using GraphPad Prism v4. Statistical analysis was performed in GraphPad Prism using a paired *t*-test. For intracranial injections, athymic mice or WT C57BL/6J mice were injected with 1×10^4 KR158 tumor cells in 1–2 μL of phosphate buffered saline into the caudate nucleus at stereotactic coordinates 2 mm lateral and 3 mm posterior to the bregma at a depth of 2 mm. Neurological symptoms developed between 55 and 78 days postinjection.

Alamar Blue Metabolic Assays and GI_{50} Calculations

The human SF295 (from NCI Division of Cancer Treatment and Diagnosis tumor cell line repository) and U87MG (ATCC cat#HTB-14) GBM lines and the mouse K1861-10, KR158, and KR130G#3 astrocytoma lines were plated at a density of 2500 cells/100 μL complete media in 96-well plates (Costar cat # 3596). Mouse primary astrocytes were plated at 5000 cells/100 μL. Cells were treated in triplicate with serial dilutions of inhibitors ranging from μM to pM. Cell proliferation was measured after 3 days using the Alamar Blue assay according to manufacterer's protocol (cat # DAL1100; Invitrogen) on a Novostar plate reader (BMG Lab Technologies). Values for 50% inhibitory concentration (IC_{50}) and 50% growth inhibitory concentration (GI_{50}) were calculated using standard procedures (described in detail in Supplementary Methods) in GraphPad Prism v4 and Microsoft Excel. IC_{50} is defined as the concentration of drug that is halfway between maximum inhibition and minimum inhibition for a given assay. GI_{50} is defined as the concentration of drug that causes 50% maximal growth inhibition. In cases where the drug does not completely block growth at maximum inhibition (Max%), the IC_{50} value will be less than the GI_{50} value. The inhibitors tested were PI-103 (cat # B-0303, Echelon Biosciences), TCN (cat # EL-332, Biomol) and rapamycin purchased from two independent sources (cat # A-275,Biomol; cat #R-5000, LC Laboratories). Antibodies against p70S6K (cat # 9202, Cell Signaling Technology) and phospho-Thr389-p70S6K (cat #9206, Cell Signaling Technology) were used to measure the inhibition of mammalian target of rapamycin (mTOR) by the drugs in Western blots.

Results

NPcis *Astrocytoma Cell Lines as an in vitro and Implantation Model of Astrocytoma*

To develop in vitro models for astrocytoma, we have generated 14 tumor lines from *NPcis* mice. To generate tumor lines from lower-grade asymptomatic astrocytomas as well as from symptomatic astrocytomas, tumor lines were cultured from defined brain regions and compared with the primary brain tumor histology in the contralateral half of the brain (Fig. 1A). Tumor lines did not grow from WT adult mouse brains but could be cultured from asymptomatic *NPcis* brains (Table 1). Out of 25 *NPcis* brains that were cultured (both symptomatic and asymptomatic), 14 gave rise to tumor lines, 4 of which were classified as low-grade astrocytoma (WHO II). Consistent with previous results,[15] all of the tumor lines showed loss of the WT copies of *Nf1* and *Trp53* (Supplemental Fig. S1) and were positive for glial fibrillary acidic protein, Nestin, Olig-1, and S-100 (Supplemental Fig. S1), consistent with glial tumors with less differentiated characteristics.

To determine whether *NPcis* astrocytoma lines were tumorigenic and whether there was a correlation between grade and tumor growth in vivo, we injected astrocytoma lines subcutaneously in immunocompromised mice (Fig. 1B and C) and orthotopically in both

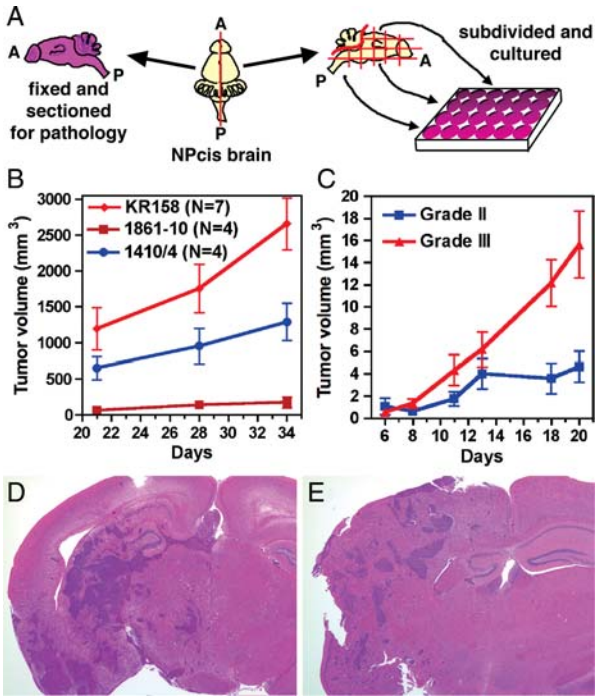

Fig. 1. Tumor cell lines isolated from both symptomatic and asymptomatic mice form tumors subcutaneously and intracranially and maintain the growth characteristics of their tumor grade. Tumor lines are isolated by cutting the dissected brain along the sagittal plane (A=anterior; P=posterior), fixing one half for histology, and dividing the other half into culture wells based on brain location (A). K1861-10 and 1410-4 are grade II astrocytomas (see Supplemental Fig. S1 for histological sections of primary tumors) and grow more slowly than the KR158 grade III anaplastic astrocytoma line (B) over a 5-week time frame. Four grade III lines (1395, K1492, K5001, and KR158) and 3 grade II lines (1410, K1861, and K4622) were injected subcutaneously, and the resulting tumor measurements over 3 weeks were averaged for grade III and grade II, showing significant differences in tumor growth (C) (Wilcoxon matched-pairs test, $P=.031$). KR158 cells on the inbred C57BL/6J background grow intracranially in both C57BL/6J (D) and immunocompromised (E) mouse brains.

syngenic C57BL6/J brains (Fig. 1D) and immunocompromised mouse brains (Fig. 1E). We observed the most aggressive growth with WHO III KR158 cells, whereas 2 low-grade WHO II tumor lines, K1861-10 and 1410-4, grew more slowly (Fig. 1B). The histology of the corresponding primary tumors for KR158, K1861-10, and 1410-4 are shown in Supplemental Fig. S1 for comparison. The average growth of 4 different grade III lines (1395, K1492, K5001, and KR158) was significantly higher than the average growth of 3 grade II lines (1410, K1861, and K4622) (Fig. 1C). Furthermore, KR158 grew invasively in syngenic C57BL6/J and immunocompromised mouse brains (Fig. 1D and E). This result demonstrates that an inbred C57BL/6J astrocytoma line is tumorigenic in mice and is not rejected by the immune system of C57BL/6J hosts.

Primary Astrocytomas and Tumor Lines from NPcis *Mice Express EGFR and PDGFRα Similar to Human Astrocytoma/Glioblastoma*

Because of the importance of EGFR and PDGFR in defining subtypes of human GBM and because many of the current experimental therapeutics focus on blocking these receptors, we examined the expression levels of EGFR and PDGFRα in primary *NPcis* astrocytomas by immunohistochemistry. In a cohort of 23 tumors, 22 were positive for PDGFRα (Fig. 2). Three tumors were strongly positive for EGFR (Fig. 2), and an additional 7 had weak EGFR expression. To confirm that the EGFR+ and PDGFRα+ cells included tumor cells (rather than only trapped or invading stroma cells), the primary tumors were costained with the proliferation marker Ki67. Proliferating cells with atypical nuclei were positive for EGFR (12% of Ki67+ nuclei) or PDGFRα (32% of Ki67+ nuclei) (Fig. 2B and C). Because Ki67 stains only a subset of tumor cells that are actively cycling, it is difficult to assess whether all tumor cells express EGFR or PDGFRα. There is currently no immunohistochemical marker that definitively differentiates tumor cells from nontumor cells in astrocytoma, so at this time we can only conclude that a subset of tumor cells (as marked by Ki67) also express EGFR or PDGFRα. A human brain tumor tissue array was stained for EGFR and PDGFRα using the same staining conditions (data not shown). Seven of the 17 GBMs (41%) were positive for EGFR expression, with no staining in lower-grade astrocytomas. The single grade II (100%) GBM, 3 of the 4 grade III (75%) GBMs, and 13 of the 17 GBMs (77%) were positive for PDGFRα expression. Six of the GBMs (35%) were positive for both EGFR and PDGFRα expression. These results demonstrate that astrocytomas and GBMs from *NPcis* mice share similar expression patterns of EGFR and PDGFRα overexpression with human astrocytomas and GBMs.

We further examined the expression of EGF and PDGF receptor and ligand family members in tumor lines and correlated the levels to tumor grade of the corresponding primary tumor. Most of the tumor lines examined showed expression of EGFR and PDGFRα (Fig. 3A) by Western blot. WT and *NPcis* astrocytes showed robust expression of EGFR (Fig. 3B), whereas PDGFRα was not detected (Fig. 3C). Because we found occasional PDGFRα+ cells in WT brain sections (Fig. 2) but no detectable EGFR, the in vitro results suggest that EGFR expression may be induced in cultured glial cells (perhaps as a result of being induced to proliferate), whereas PDGFRα expression is upregulated in tumor cells. In contrast, the ligands for PDGFR were highly expressed in both cultured astrocytes and all tumor lines by reverse transcriptase–PCR, whereas only a subset of EGFR ligands were upregulated in tumor lines relative to primary astrocytes (Fig. 3D). Amphiregulin (Areg) and betacelulin (Btc) were more highly expressed in tumor lines compared with primary astrocytes. In contrast, EGF ligand was undetectable in either primary astrocytes or tumor

Table 1. Characteristics of tumor cell lines and associated brain tumors

ID	Strain	Sex	Age (Mo)	Grade	Cis Parent	EGFR West[a]	PDGFR West[a]	EGFR IHC[b]	PDGFR IHC[b]	Location of tumor cell line growth[c]
1410	129	F	7.0	II	father	+	+++	−	+	HT, DF
1405	129	F	6.3	II/III	father	++	++	+	+	HT
K3558	129	F	6.5	NA	father	ND	ND	ND	ND	CB, HT, VF
1395	129	F	7.2	III	father	++++	+	++	+	HT
K1861	B6	M	4.9	II	father	++	++	−	+	CB, M, BS, VF, OB
K2797	B6	F	5.3	NA	father	+++		ND	ND	CC, HT, F
K4820	B6	M	6.3	NA	father	+++		ND	ND	TH, HT, F, CC
K5001	B6	F	7.9	III	father	+	+	ND	ND	TH, CC, VF
K1491	B6	F	6.2	II	mother	ND	ND	−	+	HT
K4622	B6	M	9.2	II	mother	++	+	ND	ND	F
K1492	B6	F	6.2	III	mother	++	+++	+	+	CC, HT, OB
KR158	B6	F	8.2	III	mother	+++	+++	ND	ND	WB*
KR129	B6XCBA	F	7.8	II/III	father	+++	+++	ND	ND	WB*
KR130	B6XSJL	M	8.2	IV	father	+++	+++	ND	ND	WB*

NA, not available; ND, not determined.
[a]EGFR West and PDGFR West indicate staining levels in Western blots of tumor cell lines.
[b]EGFR IHC and PDGFR IHC indicate staining levels by immunohistochemistry of primary tumor sections.
[c]HT, hypothalamus; DF, dorsal forebrain; CB, cerebellum; VF, ventral forebrain; M, medulla; BS, brain stem; OB, olfactory bulb; CC, cerebral cortex; F, forebrain; TH, thalamus; WB*, whole brain was used for culture, and then lines were cloned at limiting dilution.

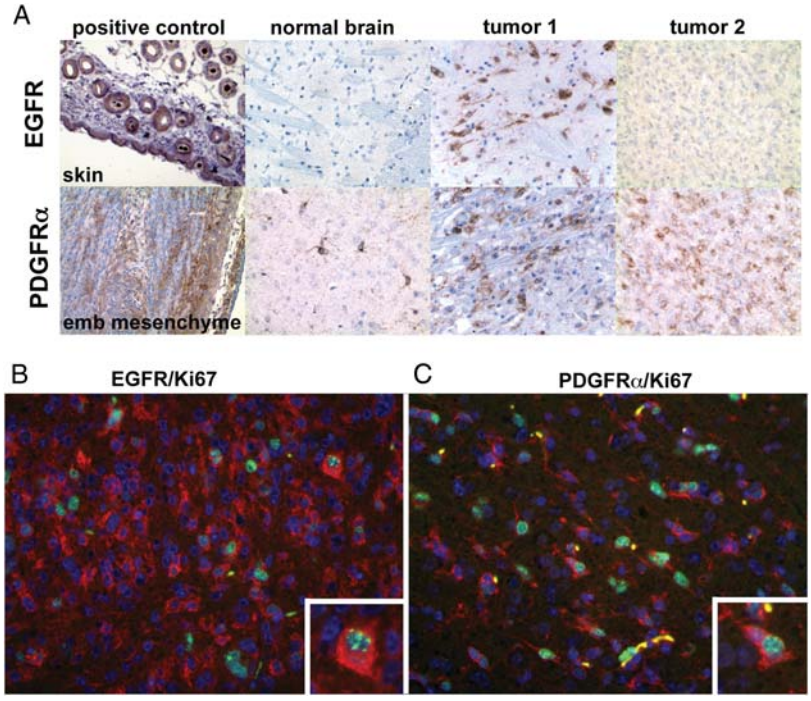

Fig. 2. Detection of EGFR and PDGFRα in primary murine astrocytomas. Top panel (A) shows DAB staining for EGFR (top row) and PDGFRα (bottom row). The first column shows positive control tissue for each antibody (EGFR = skin; PDGFRα = embryonic mesenchyme). The second column shows staining of normal brain with each antibody. The third column shows an example of a tumor that was positive for both EGFR (top) and PDGFRα (bottom). The fourth column shows an example of a tumor that was negative for EGFR (top) and positive for PDGFRα (bottom). EGFR (red) (B) or PDGFRα (red) (C) co-expresses with the proliferation marker Ki67 (green) in murine astrocytomas. Two *NPcis* littermates developed brain tumors and were euthanized on the same day. One tumor showed high expression of EGFR (B), whereas the other showed high expression of PDGFRα (C). Atypical cells and proliferating (Ki67+) cells (inset) stain for the receptors, demonstrating that tumor cells rather than only normal surrounding stroma cells are overexpressing the receptors.

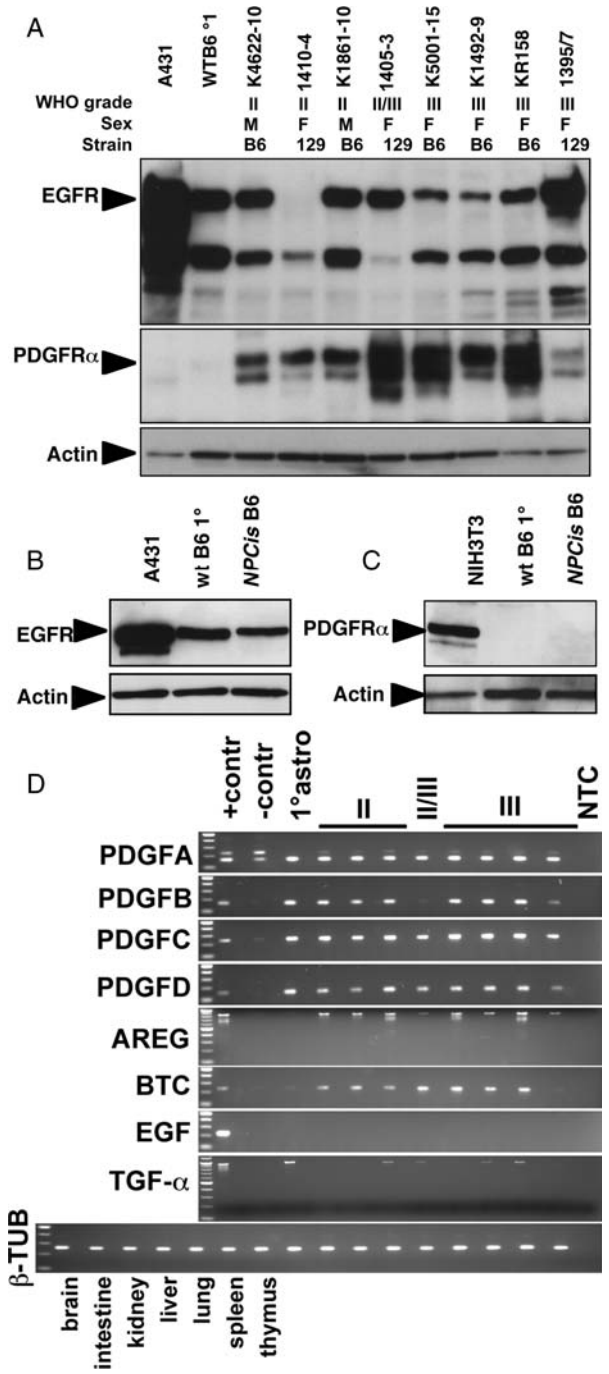

Fig. 3. Expression in astrocytoma cell lines of PDGFR and EGFR by Western blot and ligands by RT-PCR. Astrocytoma cell lines express EGFR and PDGFRα (A). Cultured primary astrocytes express EGFR (B) but not PDGFRα (C). Astrocytoma cell lines express PDGFR ligands (PDGFa, PDGFb, PDGFc, and PDGFd) as well as EGFR ligands (Areg and Btc, as well as Tgfα to a lesser extent) (D). Astrocytoma cell line order is the same in (A) and (D). *Samples:* Astrocytoma grade II: K4622-10, 1410-4, K1861-10; Astrocytoma grade II/III: 1405-3; Astrocytoma grade III: K5001-15, K1492, KR158, 1395-7. Primary astrocytes from wt B6 mice: wt B6 1°; primary astrocytes from *NPcis* B6 mice: *NPcis* B6. *Western blot controls*: A431 cells are a positive control for EGFR (A and B), and NIH3T3 cells are a positive control for PDGFRα (C). Actin is the control for equal loading of lysates (A–C). *RT-PCR controls*: positive controls (+contr) are organ samples with high expression of the ligand; negative controls (-contr) are organ samples with low levels or no expression of the ligand (PDGFa was strongly expressed in all organs tested). β-tubulin is control for template levels. No template control: NTC. PDGFa: positive control=lung, negative control=thymus; PDGFb: postive control=brain, negative control=liver; PDGFc: postive control=brain, negative control=liver; PDGFd: postive control=brain, negative control=liver; Areg: positive control=intestine, negative control=brain; Btc: positive control=brain, negative control=spleen; Egf: positive control=kidney, negative control=brain; Tgfα: positive control=brain, negative control=spleen.

lines, whereas Tgfα was expressed by cultured astrocytes, but only expressed at low levels in a subset of tumor lines.

Taken together, staining of primary *NPcis* tumors and protein expression in the derived tumor lines are consistent with tumor lines maintaining the expression of RTKs found in the primary tumors. The tumor lines show more consistent expression of EGFR than the primary tumors, which generally show rare EGFR+ cells, suggesting the selection of EGFR+ cells cultured from tumors. Given that current clinical results targeting EGFR and PDGFR have not shown conclusive patient benefit, we examined downstream signaling pathways that may be better targets in EGFR+ and PDGFR+ brain tumors, specifically the Akt and MAPK pathways.

Activation of Akt and Mapk Signaling is Necessary for Tumor Cell Proliferation, Anchorage-Independent Growth, and Migration in Mouse Astrocytoma Cells in Response to EGF and PDGF-AA

We stimulated *NPcis* astrocytoma cells with 0.1 to 10.0 ng/mL of EGF or PDGF-AA and confirmed that the Akt and MAPK pathways are activated by EGFR and PDGFR signaling in *NPcis* astrocytoma cell lines (Fig. 4 and Supplemental Fig. S2). We blocked the Akt pathway with 20 μM of PI3K-specific inhibitor LY294002 and the MAPK pathway with 10 μM of MEK-specific inhibitor U0126 (Fig. 4A) and found that phosphorylation of Akt and MAPK was blocked in all of the tumor lines regardless of differences in strain background or tumor grade. At the concentrations used, the PI3K inhibitor did not block MEK signaling, and the MEK inhibitor did not block PI3K signaling, as expected.

To determine the role of Akt and/or MAPK pathways in mitogenic signaling in mouse *NPcis* astrocytoma cells, we performed proliferation assays with ligands plus specific inhibitors of PI3K or MEK (Fig. 4B). KR158 proliferation in response to EGF or PDGF-AA was strongly reduced when the cells were treated with 20 μM of LY294002. However, cells treated with U0126 showed more moderate inhibition, suggesting differential effects of these two pathways on astrocytoma proliferation. In the absence of 1% serum, EGF

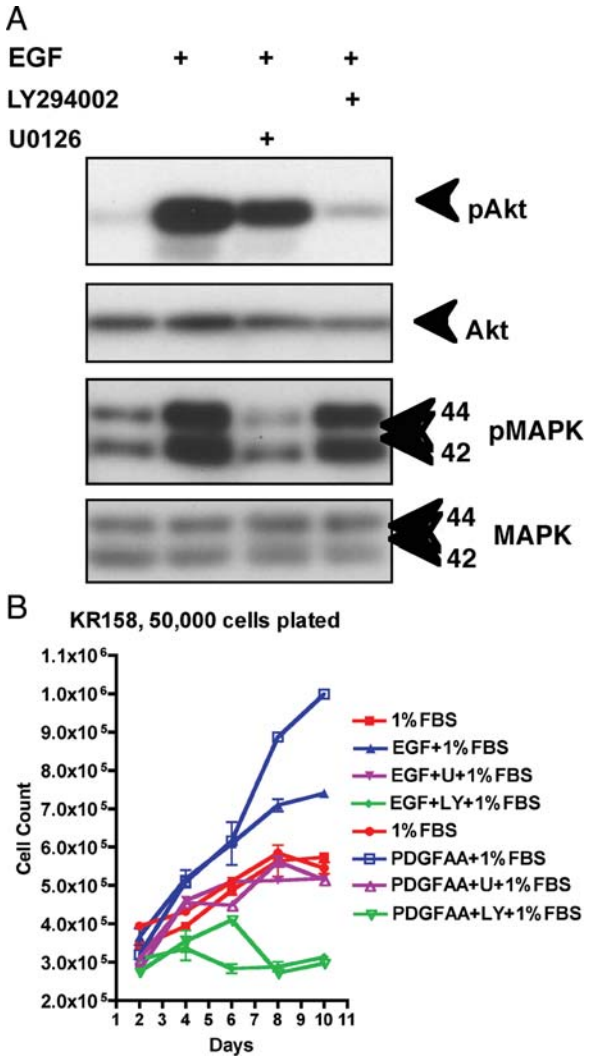

Fig. 4. LY294002 (LY) blocks phosphorylation of Akt-Ser473 (pAkt) downstream of PI3K, whereas U0126 (U) blocks phosphorylation of MAPK (p44/42 Thr202/Tyr204) (pMAPK) downstream of MEK in response to EGF signaling in KR158 cells as detected by Western blot (A). LY and U block proliferation of KR158 cells in response to either EGF or PDGF-AA (B). LY inhibits cell proliferation below basal levels of 1% serum, whereas U inhibits cells back to the basal level.

alone was insufficient to stimulate proliferation of KR158 cells, whereas in the presence of 10% serum, EGF showed no additive effect on proliferation. K1861-10, 1395-7, and 1410-4 showed similar proliferative responses to EGF and PDGF-AA in 1% serum (data not shown). In addition, we did not observe any additive or synergistic effect when both EGF and PDGF-AA were added to tumor cell cultures together (data not shown).

We confirmed that Akt and MAPK signaling has similar effects on cell transformation and migration in *NPcis* astrocytoma cells as on mitogenesis. We performed soft agar assays (Supplemental Fig. S3) to evaluate anchorage-independent growth of astrocytoma cells in response to 50 ng/mL EGF or PDGF-AA alone, or together with 20 μM of LY294002 or 10 μM of U0126. As in the mitogenesis assay, colony formation stimulated by EGF or PDGF-AA was inhibited most strongly with LY294002 and to a lesser extent with U0126 (Supplemental Fig. S3).

Next we tested the effect of EGF or PDGF-AA on astrocytoma cell motility by performing 18-hr time-lapse microscopy wound-healing experiments in the absence of serum with either 12 ng/mL ligand alone, or ligand with LY294002 (20 μM) or U0126 (10 μM) (Supplemental Fig. S3; Supplemental Movies S1–S3). Cell motility was blocked by LY294002 or U0126, with LY294002 inhibiting more strongly than U0126. To distinguish between increased cell proliferation pushing cells into the wound area and active cell migration, we mixed EGFP-labeled KR158 cells at a ratio of 1/20 to observe individual cell division and migration. Over the course of 18 hrs, cells did not divide more than once, and were seen to actively move in the direction of the wound (Supplemental Movies S1–S3).

Our results show that both EGF and PDGF-AA are sufficient to stimulate growth and migration of *NPcis* mutant astrocytoma cells and that both the PI3K and MEK signaling pathways are necessary for the full activity of these tumor cell phenotypes. Because inhibition of the PI3K pathway was consistently better at blocking tumor cell proliferation, anchorage-independent growth, and migration more completely than MEK pathway inhibitors, we next focused on the effects of additional inhibitors of the PI3K/Akt/mTor pathway to determine which steps in this pathway are the most effective targets for inhibiting *NPcis* astrocytoma cells.

Inhibition of PI3K and Akt, but not mTor Signaling Alone, Blocks NPcis *Astrocytoma Cell Proliferation*

We used our in vitro system to test inhibitors of the Akt/mTor signaling pathway that are already in clinical development for other diseases,[18–22] as well as the PI3K/mTOR dual inhibitor PI-103, which has a similar mechanism to drugs currently in clinical trials. The Alamar Blue assay for metabolic activity was used as a surrogate for proliferation, to allow measurement in a 96-well format. To determine whether inhibitors affected different tumor grades to a different extent, we assayed 3 different grades of mouse astrocytoma tumor lines, K1861-10 (WHO II), KR158 (WHO III), and KR130 (WHO IV) and compared the extent of inhibition to 2 human GBM tumor lines, SF295 and U87MG, and primary mouse astrocytes. We looked for inhibitors with GI_{50} values in the submicromolar range and a log-fold stronger inhibition of tumor cells when compared with primary astrocytes. Of 8 drugs tested (chloroquine, nelfinavir, OSU03012, PIA6, perifosine, triciribine [TCN], PI-103, and rapamycin (Y. Connell-Albert, unpublished data)), only TCN and PI-103 showed strong inhibitory activity in the nM-μM GI_{50} range (Table 2). PI-103, a dual inhibitor of Akt and mTor, showed good efficacy against all cell

Table 2. IC_{50}, GI_{50}, and maximum percent inhibition of compounds in different cell lines

Inhibitor		Astrocytes Mouse Normal	K1861 Mouse Grade II	KR158 Mouse Grade III	KR130 Mouse Grade IV	SF295 Human Grade IV	U87MG Human Grade IV	pAKT/pS6K
PI-103	IC_{50}	3.12 μM	0.80 μM	0.59 μM	0.62 μM	0.80 μM	0.63 μM	0.005 μM
	GI_{50}	5.15 μM	0.97 μM	0.66 μM	0.68 μM	0.89 μM	1.10 μM	
	Max%	83.3	95.4	86.8	94.8	94.6	86.0	100
TCN	IC_{50}	5.33 μM	0.70 μM	0.31 μM	0.74 μM	0.75 μM	27.67 μM	0.13 μM
	GI_{50}	13.58 μM	1.73 μM	0.36 μM	1.07 μM	0.99 μM	NA	
	Max%	70.7	69.0	87.1	82.3	85.9	43.2	98
Rapamycin	IC_{50}	NA	NA	0.26 nM	0.47 nM	0.35 nM	0.58 nM	<1 pM
	GI_{50}	NA	NA	NA	NA	NA	119.03 nM	
	Max%	NA	NA	33.6	45.6	46.6	50.6	100

NA, not available.

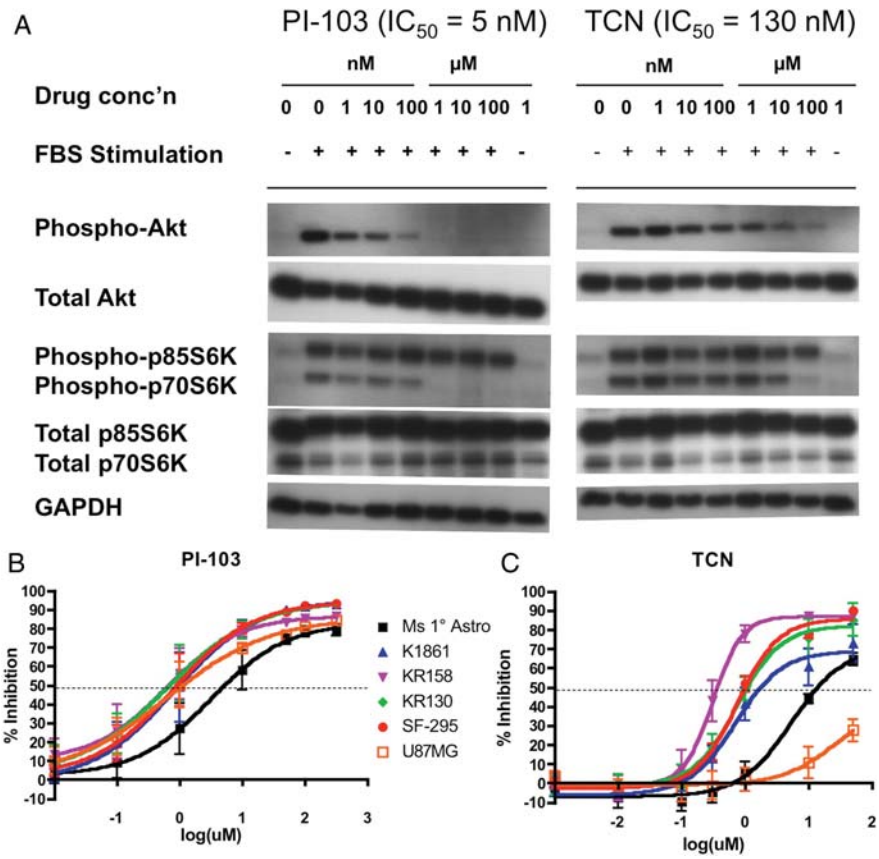

Fig. 5. Inhibition of phospho-Akt (Ser473) and phospho-p70S6K (Thr389) by increasing concentrations of PI-103 or TCN (A). KR158 cells were starved and then stimulated with 10% FBS in the presence of different concentrations of PI-103 (left panels) or TCN (right panels). Growth inhibition curves as a function of drug concentration for PI-103 (B) and TCN (C). Data points are the averages of a minimum of 8 experiments with triplicate samples in each, and standard error is shown by error bars. Averaged data were used to fit the curve for each astrocytoma cell line. Murine primary astrocytes: Ms 1 Astro; murine astrocytoma grade II: K1861; murine astrocytoma grade III: KR158; murine GBM grade IV: KR130; human GBM grade IV: SF-295 and U87MG.

lines tested, with less inhibitory effect on primary astrocytes (GI_{50}=5.15 μM) when compared with astrocytoma lines (average GI_{50}=0.86 μM) (Fig. 5). PI-103 reaches maximum inhibition around 10 μM, consistent with data that phosphorylation of both Akt (downstream of PI3K) and p70S6K (downstream of mTor) are inhibited to basal levels at 1 μM of PI-103 (IC_{50}=5 nM) (Fig. 5, Supplemental Fig. S4A). The Akt

inhibitor TCN did not effectively inhibit the human cell line U87MG but inhibited other astrocytoma cell lines in a grade-dependent manner (Fig. 5). The WHO II K1861-10 line was incompletely inhibited (69% maximum inhibition) with a GI_{50} value of 1.7 μM for TCN, whereas higher-grade tumor lines (KR158, KR130, and SF295) were inhibited to a greater extent (>80% maximum inhibition) at lower GI_{50} values (0.4–1.1 μM). Importantly, TCN was much less effective at inhibiting primary astrocytes (GI_{50}=13.6 μM), suggesting that this inhibitor may show specificity for tumor cells. TCN exhibits maximum growth inhibition around 1–10 μM and inhibits phosphorylation of Akt, as well as downstream p70S6K, to basal levels at 100 μM (IC_{50}=130 nM) (Fig. 5, Supplemental Fig. S4B). While the mTOR inhibitor rapamycin showed growth inhibitory activity in the pM-nM range (Fig. 6) as well as inhibition of phosphorylation of p70S6K at levels as low as 1 pM (Fig. 6, Supplemental Fig. S4C), the effect on inhibition of cell proliferation was always incomplete and variable, with maximum growth inhibition in the range of 30%–50% for tumor cells (Fig. 6), suggesting that mTOR inhibition alone is not sufficient to inhibit cell growth. The effects of PI-103, TCN, and rapamycin on cell growth and target inhibition are summarized in Table 2.

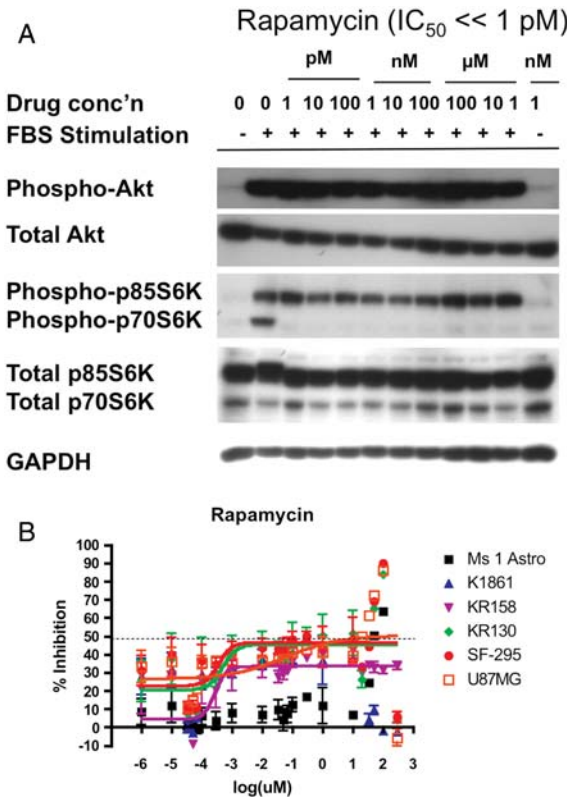

Fig. 6. Inhibition of phospho-p70S6K (Thr389) by increasing concentrations of rapamycin (A). KR158 cells were starved and then stimulated with 10% FBS in the presence of different concentrations of rapamycin. Growth inhibition curves as a function of rapamycin (B). Rapamycin showed highly variable results, with inhibition even at very low concentrations, such that data did not show a sigmoidal dose response. Murine primary astrocytes: Ms 1 Astro; murine astrocytoma grade II: K1861; murine astrocytoma grade III: KR158; murine GBM grade IV: KR130; human GBM grade IV: SF-295 and U87MG.

Discussion

We demonstrate here that mouse models of cancer can develop secondary genetic/gene expression changes (e.g., EGFR and PDGFRα overexpression) similar to those seen in human tumors that are distinct from the genetically engineered event (*Nf1* and *Trp53* mutation). This suggests that these changes are conserved across species and are critical for tumor formation. This also highlights the need to fully characterize mouse models of human cancers, as they may have even more in common molecularly with human tumors than the targeted mutations. This characterization will facilitate cross-species comparisons, as vast amounts of human data become available from efforts such as The Cancer Genome Atlas.[23] Relevant mouse models can help provide a filter to focus on the most basic and universally relevant changes in cancer, helping to make sense of complex data from human populations.

In our analysis of the expression of EGF and PDGF family receptors and ligands in astrocytomas, we find that PDGFR is upregulated in tumor cells compared with normal astrocytes, whereas ligands are universally expressed in both tumor and normal cells. In contrast, EGFR is highly expressed in both tumor cells and primary astrocytes, whereas the EGFR ligands Areg, Btc, and Tgfα are expressed at higher levels in tumor cells than in normal astrocytes. This suggests that normal cells are deficient for one of the components of an autocrine loop (PDGFRα or EGFR ligands) but that tumor cells upregulate the deficiency, making cells more sensitive to autocrine signaling.

We have generated a panel of 14 astrocytoma lines from both susceptible and resistant genetic and epigenetic backgrounds to find differences that correlate to susceptibility. At the level of EGF and PDGF family receptors and ligands, we have not yet found clear differences correlating with background susceptibility. This may be explained if the background effects responsible for susceptibility differences are developmental or non–cell autonomous, such that the tumor cells themselves are similar but the environment in which they form or propagate affects susceptibility. It is also possible that removing tumor cells from the animal and placing them in a supportive in vitro culture environment masks any differences that exist between astrocytomas from susceptible and resistant strains. Alternatively, the molecular pathways important for differences between susceptible and resistant mice may be separate from pathways that we have examined here. These lines will be an important tool for examining potential differences using more unbiased genomic and proteomic approaches.

Our results suggest that the PI3K/Akt pathway is a promising target for therapeutic intervention in *NF1* and *TP53* mutant astrocytomas, although further studies are needed to confirm these results in vivo and in patients. Several candidate therapeutics known to block Akt signaling were found to block astrocytoma growth, with PI-103 and TCN found to be the most promising due to high sensitivity and tumor-specific effects. TCN is currently in phase I trials (http://clinicaltrials.gov/) for other tumor types, and our results suggest that this drug may also be effective against astrocytoma, specifically those carrying mutations in *NF1* and/or *TP53*. TCN was identified in our high-throughput screen of the NCI diversity set library[17] as a compound that showed cytostatic effects with borderline cytotoxicity. Early clinical studies with TCN in the 1980s–1990s showed very limited effect of TCN on metastatic disease even at dose-limiting toxicity.[24,25] Because the ability of TCN to inhibit Akt was not understood at the time, these trials may not have shown efficacy due to a lack of Akt dependence of the tested tumors. A current phase I trial of TCN in metastatic cancers (NCT00363454) takes the phosphorylation status of Akt in the tumor into account and may show better efficacy. Due to toxicity issues associated with high doses of TCN, it may be critical to conduct targeted clinical trials with this compound and use doses of TCN that inhibit Akt in tumors with high levels of Akt phosphorylation to balance efficacy against toxicity.

PI-103 is a dual inhibitor of PI3K (upstream of Akt) and mTOR (downstream of Akt) and has been shown to inhibit human glioma cells.[26,27] We have extended these findings specifically to astrocytomas carrying mutations in *Nf1* and *Trp53* and have shown that PI-103 may have a promising therapeutic index, as evidenced by the comparison of normal primary astrocytes with tumor cells. PI3K/mTOR dual inhibitor compounds (BGT226 and BEZ235A) are currently in phase I/II trials for other cancers, and it will be interesting to determine whether all PI3K/mTOR inhibitors have similar efficacy against *Nf1;p53* mutant astrocytomas. Our results, taken together with others,[26,27] support the use of these therapies for astrocytoma/GBM.

We tested several compounds that are believed to inhibit PI3K/Akt signaling directly or indirectly, and although they did show dose-responsive inhibitory effects (Y.S.C.-A. and K.M.R., unpublished data), inhibition required relatively high concentrations of the compounds, consistent with indirect activity on the signaling pathway. Nelfinavir, chloroquine, and perifosine, which are currently in clinical trials for GBM or other gliomas, did not seem to be as promising in our assays as TCN and PI-103. Nelfinavir, chloroquine, and perifosine are in clinical trials as combination therapies, and it may be that in combination with other drugs or radiation therapy[20,21] they will hold more promise for gliomas.

Rapamycin, along with other mTOR inhibitors, is currently in clinical trials in combination therapy against brain tumors. We found that rapamycin was not as effective at inhibiting *Nf1;p53* mutant astrocytomas as more upstream compounds inhibiting PI3K and Akt. Although rapamycin slowed cell growth, it was not able to stop astrocytoma proliferation, regardless of the concentration used. In many (but not all) experiments, the response to rapamycin was not concentration dependent, showing a bimodal response in some experiments or similar inhibition at all concentrations tested down to 1 pM. This suggests that rapamycin may have multiple cellular targets for inhibition. To confirm that this effect was not batch dependent, we tested rapamycin purchased from two different suppliers and found similar results. Other studies have examined the effects of rapamycin or rapamycin analogues on different *Nf1* mutant nervous system tumors. Rapamycin inhibits *Nf1*−/− astrocytes at relatively high concentrations (1 μM), although GI_{50} values were not calculated.[28] Similarly, high concentrations (20 mg/kg) of rapamycin were shown to inhibit the growth of *Nf1*−/− optic nerve gliomas in vivo.[29] Studies of *Nf1*−/− malignant peripheral nerve sheath tumors (MPNSTs) showed more sensitivity of these cells to rapamycin in vitro ($IC_{50} < 10$ nM) and in vivo (inhibition at 5 mg/kg).[30] Similar studies with a rapamycin analog also showed similar sensitivity of MPNST cells with 10 nM giving a 50% reduction in growth in vitro and 10 mg/kg preventing the growth of tumors in vivo.[31] These various studies suggest that although rapamycin inhibits cell growth of *Nf1*−/− nervous system tumor cells, inhibition does not approach 100% in vitro, and the effects in vivo may be due more to an effect of rapamycin on angiogenesis, or other off-target effects, than on the tumor cells themselves.[31] Thus, our data, taken together with other data, suggest that rapamycin may play an important role as a therapy in vivo in combination with other drugs but is not as effective as inhibitors of the upstream PI3K/Akt signaling pathway at inhibiting growth of astrocytoma cells directly.

It is important to note that one of the cell lines tested (K1861) was derived from a grade II astrocytoma found in an asymptomatic mouse and was very slow growing in subcutaneous xenograft models (Fig. 2). This line showed partial response to TCN (maximum inhibition=69%; Table 1), similar to primary astrocytes, but full response to PI-103 (maximum inhibition=95%; Table 1), similar to GBM cells. This suggests that the stage of tumorigenesis, and hence the accumulated mutations, may be important in the response to therapy, highlighting the advantages of testing therapies in a broad range of tumor cells. It is possible that as astrocytomas progress to higher grades, they become more reliant on single oncogenic pathways (oncogene addiction), as opposed to branched oncogenic pathways, and therefore can be more effectively inhibited by single inhibitor agents, whereas early-stage tumors require inhibition of more diverse pathways. Additional studies in asymptomatic tumors are needed to fully explore these possibilities, but this distinction has important implications when applying drugs that have been developed in end-stage patients to patients who are newly diagnosed.

Our in vitro tumor cell models have been developed from a mouse model of the malignancies associated with *NF1*. Although we have focused on astrocytomas and GBMs, it is possible that the therapeutics studied here may also have broad application to *NF1* patients. Additional studies are needed to examine whether TCN and PI-103 are candidate therapeutics for other *NF1* malignancies, such as MPNSTs, pheochromocytomas, and myeloid leukemia, as well as more benign tumors, such as neurofibromas and optic nerve gliomas. In this regard, PI-103 may be particularly interesting to pursue, given its activity against grade II astrocytoma, as compared with the incomplete activity of TCN.

We demonstrate here that inhibition of the PI3K/Akt signaling pathway is very effective at blocking growth of astrocytoma cells. This does not exclude the MEK/MAPK pathway as a potential therapeutic target, but suggests that MEK/MAPK inhibition alone is not sufficient and may need to be combined with inhibitors of other pathways to fully block tumor growth. We find that the MEK inhibitor U0126 inhibits cells to levels seen in the absence of EGF or PDGFα stimulation. However, there may be factors either found in serum or produced by the tumor cells in an autocrine fashion that stimulate cells through MEK/MAPK-independent pathways.

As more is learned about specific molecular alterations in human cancers, it is important that the development of appropriate models keeps pace. We present here the development and characterization of tumor lines from grade II through IV *Nf1;p53* astrocytomas that can be used to better understand the signal transduction pathways underlying certain astrocytoma and GBMs, as well as malignancies associated with *NF1*. We show that these tumor cells may develop autocrine signaling pathways through the upregulation of PDGFRα and ligands for EGFR and that the PI3K/Akt signaling pathway is particularly important for tumor cell phenotypes, such as proliferation, migration, and anchorage-independent growth. By comparing tumor lines with primary astrocytes, we find that TCN and PI-103 show particular promise as sensitive inhibitors of the PI3K/Akt/mTOR signaling pathway that demonstrate specificity for tumor cells. Further analysis of these tumor lines may help in the understanding of cell-autonomous differences in tumors from susceptible and resistant individuals.

Supplementary Material

Supplementary material is available online at *Neuro-Oncology* (http://neuro-oncology.oxfordjournals.org/).

Acknowledgments

We thank Alma Arnold and the Optical Imaging Lab (SAIC-Frederick), Isaac Mizrahi, Alex Kiener, Kristi Fox, and Chris Perella for technical assistance, and Keiko Akagi, Phil Dennis, Stephen Lockett, Lino Tessarollo, Ira Daar, and Doug Lowy for helpful discussions and comments on the manuscript. This research was supported by the Intramural Research Program of the NIH, NCI.

Conflict of interest statement. None declared.

Funding

This research was supported by the Intramural Program of the NIH, NCI.

References

1. CBTRUS. Central Brain Tumor Registry of the United States: Statistical Report: Primary Brain Tumors in the United States, 2000–2004. Hinsdale, IL: Central Brain Tumor Registry of the United States; 2008.
2. Arko L, Katsyv I, Park GE, Luan WP, Park JK. Experimental approaches for the treatment of malignant gliomas. *Pharmacol Ther.* 2010;128:1–36.
3. Rich JN, Reardon DA, Peery T, et al. Phase II trial of gefitinib in recurrent glioblastoma. *J Clin Oncol.* 2004;22:133–142.
4. Wen PY, Yung WK, Lamborn KR, et al. Phase I/II study of imatinib mesylate for recurrent malignant gliomas: North American Brain Tumor Consortium Study 99-08. *Clin Cancer Res.* 2006;12:4899–4907.
5. Haas-Kogan DA, Prados MD, Tihan T, et al. Epidermal growth factor receptor, protein kinase B/Akt, and glioma response to erlotinib. *J Natl Cancer Inst.* 2005;97:880–887.
6. Mellinghoff IK, Wang MY, Vivanco I, et al. Molecular determinants of the response of glioblastomas to EGFR kinase inhibitors. *N Engl J Med.* 2005;353:2012–2024.
7. Furnari FB, Fenton T, Bachoo RM, et al. Malignant astrocytic glioma: genetics, biology, and paths to treatment. *Genes Dev.* 2007;21:2683–2710.
8. Cai WW, Chen R, Gibbs RA, Bradley A. A clone-array pooled shotgun strategy for sequencing large genomes. *Genome Res.* 2001;11:1619–1623.
9. Li J, Yen C, Liaw D, et al. *PTEN*, a putative protein tyrosine phosphatase gene mutated in human brain, breat, and prostate cancer. *Science.* 1997;275:1943–1947.
10. Lee JW, Soung YH, Kim SY, et al. PIK3CA gene is frequently mutated in breast carcinomas and hepatocellular carcinomas. *Oncogene.* 2005;24:1477–1480.
11. Mizoguchi M, Betensky RA, Batchelor TT, Bernay DC, Louis DN, Nutt CL. Activation of STAT3, MAPK, and AKT in malignant astrocytic gliomas: correlation with EGFR status, tumor grade, and survival. *J Neuropathol Exp Neurol.* 2006;65:1181–1188.
12. Levine A. p53, the cellular gatekeeper for growth and division. *Cell.* 1997;88:323–331.

13. McLendon R, Friedman A, Bigner D, et al. Comprehensive genomic characterization defines human glioblastoma genes and core pathways. *Nature.* 2008;455:1061–1068.
14. Parsons DW, Jones S, Zhang X, et al. An Integrated Genomic Analysis of Human Glioblastoma Multiforme. *Science.* 2008;321:1807–1812.
15. Reilly KM, Loisel DA, Bronson RT, McLaughlin ME, Jacks T. Nf1;Trp53 mutant mice develop glioblastoma with evidence of strain-specific effects. *Nat Genet.* 2000;26:109–113.
16. Reilly KM, Tuskan RG, Christy E, et al. Susceptibility to astrocytoma in mice mutant for Nf1 and Trp53 is linked to chromosome 11 and subject to epigenetic effects. *Proc Natl Acad Sci USA.* 2004;101: 13008–13013.
17. Hawes JJ, Nerva JD, Reilly KM. Novel Dual-Reporter Preclinical Screen for Antiastrocytoma Agents Identifies Cytostatic and Cytotoxic Compounds. *J Biomol Screen.* 2008;13:795–803.
18. LoPiccolo J, Blumenthal GM, Bernstein WB, Dennis PA. Targeting the PI3K/Akt/mTOR pathway: effective combinations and clinical considerations. *Drug Resist Updat.* 2008;11(1–2):32–50.
19. LoPiccolo J, Granville CA, Gills JJ, Dennis PA. Targeting Akt in cancer therapy. *Anticancer Drugs.* 2007;18:861–874.
20. Gupta AK, Cerniglia GJ, Mick R, McKenna WG, Muschel RJ. HIV protease inhibitors block Akt signaling and radiosensitize tumor cells both in vitro and in vivo. *Cancer Res.* 2005;65:8256–8265.
21. Pore N, Gupta AK, Cerniglia GJ, et al. Nelfinavir down-regulates hypoxia-inducible factor 1alpha and VEGF expression and increases tumor oxygenation: implications for radiotherapy. *Cancer Res.* 2006;66:9252–9259.
22. Pore N, Gupta AK, Cerniglia GJ, Maity A. HIV protease inhibitors decrease VEGF/HIF-1alpha expression and angiogenesis in glioblastoma cells. *Neoplasia.* 2006;8:889–895.
23. Collins FS, Barker AD. Mapping the cancer genome. Pinpointing the genes involved in cancer will help chart a new course across the complex landscape of human malignancies. *Sci Am.* 2007;296:50–57.
24. Hoffman K, Holmes FA, Fraschini G, et al. Phase I-II study: triciribine (tricyclic nucleoside phosphate) for metastatic breast cancer. *Cancer Chemother Pharmacol.* 1996;37:254–258.
25. Feun LG, Blessing JA, Barrett RJ, Hanjani P. A phase II trial of tricyclic nucleoside phosphate in patients with advanced squamous cell carcinoma of the cervix. A Gynecologic Oncology Group Study. *Am J Clin Oncol.* 1993;16:506–508.
26. Fan QW, Cheng CK, Nicolaides TP, et al. A dual phosphoinositide-3-kinase alpha/mTOR inhibitor cooperates with blockade of epidermal growth factor receptor in PTEN-mutant glioma. *Cancer Res.* 2007;67:7960–7965.
27. Fan QW, Knight ZA, Goldenberg DD, et al. A dual PI3 kinase/mTOR inhibitor reveals emergent efficacy in glioma. *Cancer Cell.* 2006;9:341–349.
28. Dasgupta B, Yi Y, Chen DY, Weber JD, Gutmann DH. Proteomic analysis reveals hyperactivation of the mammalian target of rapamycin pathway in neurofibromatosis 1-associated human and mouse brain tumors. *Cancer Res.* 2005;65:2755–2760.
29. Hegedus B, Banerjee D, Yeh TH, et al. Preclinical cancer therapy in a mouse model of neurofibromatosis-1 optic glioma. *Cancer Res.* 2008;68:1520–1528.
30. Johannessen CM, Johnson BW, Williams SM, et al. TORC1 is essential for NF1-associated malignancies. *Curr Biol.* 2008;18:56–62.
31. Johansson G, Mahller YY, Collins MH, et al. Effective in vivo targeting of the mammalian target of rapamycin pathway in malignant peripheral nerve sheath tumors. *Mol Cancer Ther.* 2008;7:1237–1245.